

Minimizing the costs of biorefinery processing by managing perennial crop age: An example from Brazilian sugarcane ethanol

Abstract

We develop and analyze an unexplored mechanism to reduce biorefinery supply chain costs when the feedstock is a perennial crop: adjusting the age-structure, and hence yield, of the perennial feedstock. The non-monotonicity of the age-yield function introduces a non-convexity to the cost-minimization problem. We show that, despite this, the problem has a solution and present analytic and numeric comparative statics, finding that smaller refineries are most likely to benefit from optimizing age-structure. The model is calibrated to the sugarcane ethanol industry in the South-Central region of Brazil and shows that the cost-reductions from optimizing age, compared to maximum sustainable yield, are on the order of one percent. Generally, the magnitude of the cost reduction will depend on the life-cycle of the crop, the costs of growing and transporting the feedstock, and the size of the biorefinery.

JEL Classification: D24, Q13, Q16

1 Introduction

Agricultural supply chains are crucial for bringing food from growers to increasingly urban populations. The particular structure of an agricultural supply chain can affect the size and distribution of returns to participants along the chain, as well as the adoption and diffusion of agricultural technologies, and has the potential to transform an economy beyond the agricultural sector (Barrett et al., Forthcoming). While these effects have long been documented by economists and effective frameworks have been developed for analyzing components of the supply chain, there are few studies that provide an “explicit framework for economic principles of supply chain design” (Zilberman, Lu, and Reardon, 2019, p. 289). Perennial crops provide multiple sources of value including food, such as fruit, nuts, cocoa, and coffee; fuel, including sugarcane ethanol and cellulosic biofuel; agronomic benefits, such as longer growing seasons and more efficient use of water (Glover et al., 2010; Wallace, 2000, p. 1638); and ecological and environmental services, such as carbon sequestration (Kreitzman et al., 2020) and erosion control (Glover et al., 2010; Molnar et al., 2013). Our paper helps fill this gap by developing a novel theoretical framework for analyzing agricultural supply chains for perennial crops, a class of crops with great economic importance worldwide and an additional constraint not present in annual crop production: older, higher-yielding plants began as younger, less-productive plants.

For agricultural firms to maximize their profitability, they must optimally design their supply chain. Du et al. (2016) decompose this decision into six components, including questions of how much feedstock and downstream services to produce in-house and how much to outsource, which technologies to use for processing, and what contracts to use for any outsourced production. Answering these questions requires a two stage model, first determining the minimal supply chain costs for a given output and sourcing arrangement, and second, choosing the profit maximizing level of output, given the minimum cost production function.

In this paper, we focus on the first stage of the supply chain design problem. Minimizing supply chain costs requires minimizing over every relevant dimension. Supply chains with perennial feedstocks have an additional constraint over annual crops: To obtain perennials of a certain age, they must be grown from younger plants. There is a relationship between age and yield. Generally, the yield increases with age, before peaking and declining (Mitra, Ray, and Roy, 1991). The unconstrained grower would wish to have a production system consisting only of plants at the maximum yielding

age. However, when incorporating the aging constraint, the yield of such a production system, in which all crops have an identical age, would vary with the relationship between age and yield. For a processor with fixed capacity, better to minimize the deterministic yield variation by keeping a portfolio of multiple of crop ages. Tisdell and De Silva (1986) show that a uniform distribution of ages eliminates any deterministic yield variation due to age and that this distribution can be described by its average age.

But which average age will minimize the supply chain costs? A natural candidate is the yield maximizing distribution identified in Tisdell and De Silva (1986). However, in this paper we show analytically that costs along the supply chain, including replanting costs, delivery costs, and processing costs, will affect the cost-minimizing age, which is generally older than the yield maximizing age. We ground this model in the context of Brazilian sugarcane ethanol production, a well-developed industry that exemplifies the perennial feedstock supply chain.

1.1 Biofuel supply chains that use perennial feedstocks

Biofuels have great potential to assist efforts in climate change mitigation due to their lower life cycle carbon emissions in comparison to gasoline (Khanna and Crago, 2012). The environmental benefits of biofuel depend on the feedstock used and the production process. In a recent meta-analysis, Hochman and Zilberman (2018) found that corn ethanol reduces greenhouse gas emissions by 11 percent compared to gasoline. In comparison, sugarcane ethanol can reduce greenhouse gas emissions by around seventy five percent (Crago et al., 2010; Manochio et al., 2017) . Cellulosic ethanol can have even greater environmental benefits, with greenhouse gas reductions up to 86 percent (Wang, 2007).

The cost of the supply chain to convert biomass into energy is one of the most important barriers to adoption (De Meyer et al., 2014; Rentizelas, Tolis, and Tatsiopoulos, 2009). Both corn and sugarcane ethanol are ‘first-generation’ technologies, where the ethanol is fermented directly from sugars in the feedstock. Cellulosic ethanol is a ‘second-generation’ technology, where non-fermentable complex compounds are first broken down into simpler sugars, which are then fermented. First generation technologies are in widespread use, with the US leading corn ethanol production and Brazil leading sugarcane ethanol production. The adoption of cellulosic ethanol has been hampered by high costs.

The feedstocks for sugarcane and cellulosic biofuels both come from perennial crops, where the feedstock may be harvested for multiple years before being replanted. Brazilian sugarcane is usually grown in a six year cycle (Margarido and Santos, 2012), while miscanthus and switchgrass, two of the most promising cellulosic feedstocks, can be grown for over 10 years before needing to be replanted (Douglas et al., 2009; Heaton, 2010).

Perennial feedstocks tend to come from the local area. Sugarcane is highly perishable after it is harvested and must be processed at the biorefinery within 24 hours of being harvested. In São Paulo, feedstock travels, on average, 20 kilometers to the biorefinery (Crago et al., 2010). Cellulosic feedstock, on the other hand, can be dried, so perishability is less of an issue, but it is bulky, making long-distance transportation a substantial cost (Malladi and Sowlati, 2018).

The quantity of feedstock available in the biorefinery’s local area will depend on two factors: the planted area and the yield per unit of land. For annual feedstocks, like corn, both the yield and area can be optimized each growing season. Perennial feedstocks, however, have yields that depend on the age of the crop, with maximum yields often being reached some years after the planting season. This imposes an additional constraint on the manager of a biorefinery that uses perennial feedstocks.

As indicated by a series of recent reviews, existing studies of biomass supply chain optimization tend to focus on optimizing the planted area (De Meyer et al., 2014; Malladi and Sowlati, 2018; O’Neill and Maravelias, 2021; Zahraee, Shiwakoti, and Stasinopoulos, 2020). The papers covered by these reviews focus on the area and the location of land to grow the feedstock to supply a local biorefinery, or network or refineries. Mostly they hold yield per unit of land constant, although some allow for heterogeneity between parcels of land and uncertainties in yield. For example, Debnath, Epplin, and Stoecker (2014) solve for the cost-minimizing land area to feed a fixed biorefinery size when yields are subject to stochastic weather shocks. O’Neill and Maravelias (2021) identify three papers where farmer decisions can influence yield through fertilization and/or harvest decisions.

1.2 Contributions of the paper

In this paper we present a framework for modeling the supply-chain for a vertically integrated biorefinery using perennial feedstocks, which can be used to minimize the costs of supplying the refinery’s feedstock needs. To our knowledge, this is the first

study that explicitly includes the optimization of the feedstock crop’s age as a control parameter. In the model, both planted area and age-structure can be chosen by the decision maker. Our analysis focuses on a particular subset of possible age-structures known as the ‘balanced orchard’. A balanced orchard has an equal proportion of land allocated to each age-class. For example, if there were only young and old trees, a balanced orchard would allocate half the land to young trees and half to old trees. Focusing on the balanced orchard allows the state of the orchard to be characterized by the average age. More generally, modeling an n -age-class orchard would need n state variables (see Mitra, Ray, and Roy (1991) for a more general discussion of possible age-structures). Furthermore, the balanced orchard minimizes the year-to-year variation in yields due to age-structure (Tisdell and De Silva, 1986), thereby avoiding the addition of another source of feedstock supply variation. Reducing this variation is an explicit goal of biomass supply chain optimization (Mafakheri and Nasiri, 2014; Sharma et al., 2013; Margarido and Santos, 2012; Debnath, Epplin, and Stoecker, 2015)

Building on the model of processed product costs by Wright and Brown (2007), we develop a model of perennial feedstock production and processing that includes maximum age as a control variable, generating a trade-off between land and yield to feed a processing facility of fixed size. We generate first order conditions for the model for a large class of yield functions and analyze the resulting comparative statics. The lower cost set for this problem is not convex, so we cannot rely on the usual conditions for a solution. We demonstrate that the first order conditions necessarily have a solution.

We use this model to show that optimal feedstock average age is older than the yield-maximizing age-structure (in contrast to Tisdell and De Silva (1986), who suggest using the maximum yield age-structure in an orchard-only context). We also show that optimal maximum orchard age declines with the scale of the biorefinery, and that biorefinery supply chain costs can be reduced by optimizing average age. We present analytical results to explain the trade-offs between average age and land. Although our analytical model abstracts away from many of the details of practical supply chains, the majority of existing models of biofuel supply chain optimization are mathematical programming models, which, while useful for analyzing policy scenarios, are less useful for illuminating the general trade-offs along the supply chain.

We calibrate the model to the sugarcane ethanol industry in the Brazilian state of São Paulo. Our simulations show results that are consistent with the model’s theo-

retical predictions, but we find that the cost savings from including the age-structure optimization are small, in the order of 0.25 percent. Using Monte Carlo simulations to explore the parameter space around the baseline calibration, we find parameter sets in the neighborhood of the Brazilian example with cost reductions up to 21 percent. However, 99 percent of simulations have cost reduction percentages of less than 1.42%. Thus, the empirical relevance of the average age optimization channel depends on the particular parameters for a supply chain. Moreover, we abstract away from the contracting process in a non-vertically integrated supply chain (cf. Alexander et al., 2012; McCarty and Sesmero, 2021). This is reasonable in the Brazilian biofuel context as approximately 70 percent of sugarcane acreage is owned and managed by mills (Sant’Anna et al., 2018).

In what follows, we first develop a theoretical model that incorporates average age, planted area, transportation, and processing. Then we identify the conditions for minimizing the cost in this model and show how the optimal planted area and average age vary with biorefinery capacity and other parameters. The theoretical results are illustrated with an example from the Brazilian sugarcane industry.

2 An Analytical Model of Perennial Age, Growing Region Area, and Processing Facility Capacity

Consider a processing facility of given size that is supplied a feedstock grown by a perennial crop in surrounding fields. Assume that this is a vertically integrated system where a single manager controls the facility, and the land and crop management for the feedstock. The manager’s problem is to minimize the cost of the feedstock to the facility by choosing how much land to use and how the feedstock is grown on that land. We pose this as a static problem for the manager, which can be interpreted as the long-run, steady-state management strategy for the facility. In this study we neither study the short run dynamics of the manager’s problem, nor the choice of facility size in the first place.

Wright and Brown (2007) observed that there are three components to the cost of producing processed product: feedstock cost at the farm gate; feedstock delivery costs; and facility operating costs. The cost minimization problem facing the manager is

$$\min \left[\begin{array}{c} \text{Farm gate} \\ \text{feedstock costs} \end{array} + \begin{array}{c} \text{Feedstock} \\ \text{delivery costs} \end{array} + \begin{array}{c} \text{Processing} \\ \text{costs} \end{array} \right] \quad \text{such that} \quad \begin{array}{c} \text{Feedstock} \\ \text{production} \end{array} = \begin{array}{c} \text{Facility} \\ \text{capacity} \end{array}$$

We discuss each of these components of cost in turn to develop a mathematical statement of the manager’s objective function.

2.1 Feedstock production

The facility requires feedstock for processing. Call the quantity of feedstock arriving at the facility Q . Feedstock production Q is the product of planted, L , and per-unit land productivity, y , i.e. $Q = y L$

2.1.1 Land productivity, y

Since the feedstock is perennial, the productivity of a single tree varies over its lifespan so the total productivity of the orchard is the weighted sum of the productivities of all the constituent trees (The term orchard should be seen as a stand-in for all perennial crops, including tree crops and perennial grasses). Let $f(a)$ —the age-yield function—be the yield per unit land of a -year-old trees.

The age-structure of the orchard through time can exhibit many different trajectories (see Mitra, Ray, and Roy (1991) for more discussion), but we restrict this analysis attention to a special type of trajectory: the balanced orchard. In a balanced orchard the distribution of tree ages follows a uniform distribution from 0 to maximum tree age, n (Tisdell and De Silva, 1986). The density of each age of tree is thus $\frac{1}{n}$. We call this an n -orchard. We call an *older* orchard one with a larger n , and a *younger* orchard one with a smaller n .

The balanced orchard is the supply-variation minimizing steady-state age-structure. There are two reasons to focus on balanced orchards. First, balancing an orchard to minimize supply variation is frequently a direct management objective for perennial crop growers and processing facility operators (Tisdell and De Silva, 1986; Margarido and Santos, 2012; Mafakheri and Nasiri, 2014; Sharma et al., 2013; Margarido and Santos, 2012; Debnath, Epplin, and Stoecker, 2015). Second, it allows us to write a simple model that can focus directly on the trade-offs between age, land, and processing facility capacity, while avoiding the technical details of transition dynamics. Because of this, our analysis must be considered a long-run equilibrium.

2.1.2 Allowable age-yield functions

We impose the following conditions on the age-yield function to ensure a analytical solution

$$f(a) \text{ is continuous} \tag{1}$$

$$f(0) = 0 \tag{2}$$

$$f(a) \text{ monotonically increases to a maximum and then monotonically decreases} \tag{3}$$

$$\lim_{a \rightarrow \infty} a f(a) = 0 \tag{4}$$

Assumption (1) aids analysis of the supply-chain optimization problem. Although continuity can only ever be an approximation of an empirical age-yield function, we consider it to be a reasonable assumption, and that it is a worthwhile price to pay to facilitate analysis. Assumption (2) requires that plants are non-yielding when they are planted. This is a reasonable assumption when considering the entire life-cycle of a plant. However, it may be possible for the manager to buy saplings that are bearing fruit when he takes possession of them. We exclude this possibility. Assumption (3) is similar to a standard assumption in the perennial crop theory literature (Mitra, Ray, and Roy, 1991), but it is a little stronger, since it excludes the possibility that trees may have a maturity phase where they produce their maximum yield for several years in a row. This assumption, however, allows the age-yield function to become arbitrarily close to this case. Assumption (4) requires that the age-yield function approaches zero ‘fast enough’ as the age of the tree approaches infinity. In particular the assumption requires that the age-yield function approach zero faster than $\frac{1}{x}$. This is clearly a reasonable assumption since the oldest known fruit tree, the olive tree of Vouves in Crete, is around 2000-4000 years old and still produces fruit (Riley, 2002). However, this assumption imposes two important modeling restrictions on the analyst. First, the age-yield function cannot approach a positive constant. This may be an attractive assumption if the tree has a long period of relatively constant yield toward the end of its life. Second, it rules out age-yield functions that approach zero too slowly. The analyst must check any candidate age-yield function against these assumptions before relying on the results of this study.

2.1.3 Feedstock production from an n -orchard

Assuming a uniform distribution of ages, for an orchard with maximum age n , the yield of feedstock per unit of land is

$$y(n) = \frac{1}{n} \int_0^n f(a) da$$

There is a trade-off between marginal and average yield inherent in this function. Since $f(a)$ is non-negative, the integral term is increasing in n . But an increase in n increases the number of age classes that the yield must be averaged across. Whether y is increasing or decreasing in n depends on the contribution of the marginal tree relative to the average at that n , which is shown by the derivative of y with respect to n .

$$\frac{dy}{dn} = \frac{1}{n} \left(f(n) - \frac{1}{n} \int_0^n f(a) da \right) = \frac{1}{n} \left(\underbrace{f(n)}_{\text{Yield of additional } n\text{-tree}} - \underbrace{y(n)}_{\text{yield of } n\text{-orchard}} \right)$$

The terms in the parentheses are multiplied by $\frac{1}{n}$ because the contribution of any single tree is diluted with an increase in the number of age-classes in the n -orchard. Let the maximum age of the uniform distribution that maximizes yield be n_{MSY} .

2.2 Age-Dependent costs

Replanting costs can be a substantial cost in perennial crop production. In an example sugarcane farm budget prepared for sugarcane growing in the South-Central region of Brazil, Teixeira (2013) found that replanting costs accounted for around 25 percent of the annual operating cost of a 5-orchard. If C_n is the cost of replanting trees on a unit of land, $\frac{C_n}{n}$ is the annual replanting cost of an n -orchard, since only $\frac{1}{n}$ of the trees are replanted each year.

2.3 Age-Independent costs

Some fraction of the farm-gate costs must be incurred per unit land, regardless of the age of the trees on it. This will include the manager's time, the rental rate of the land, any irrigation infrastructure etc. Since this cost is *fixed* relative to the age of the trees, it is denoted C_f .

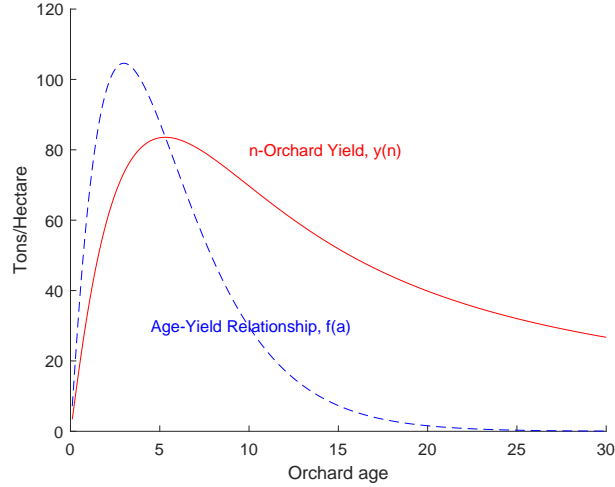


Figure 1: Yield is increasing in n while the marginal age class, n , is more productive than the average of the n -orchard, $y(n)$.

2.4 Total land, L

The other component determining total feedstock quantity is the area of land controlled by the manager, L . The choice of L determines how many units of land have a perennial feedstock orchard with yield $y(n)$ on them. This determines total feedstock production, $Q = y(n) L$, and total feedstock growing costs, $L (C_f + \frac{C_n}{n})$.

2.5 Delivery costs

The total quantity of land also affects the cost of transporting the feedstock from the farm gate to the processing facility (Wright and Brown, 2007). Delivery costs are proportional to the quantity of feedstock multiplied by the average delivery distance.

The average delivery distance is increasing in the area of land around the facility. In the case of a facility surrounded by a circular growing region, following Overend (1982), the distance from the facility to the furthest field is given by

$$L = \pi r_{max}^2 \Rightarrow r_{max} = \sqrt{\frac{L}{\pi}}$$

The area-weighted average delivery distance is $r_{av} = \frac{2}{3}r_{max}$. We express delivery costs as $C_D y(n)L^\alpha$ (or $C_D Q L^{\alpha-1}$), where $\alpha > 1$. Hence delivery costs are a convex function of growing region area. If the growing region is not circular, α is not necessarily equal to $\frac{3}{2}$, but delivery costs still increase as a convex function of land (see appendix B.1 for full derivation).a

We make a distinction between the area of land planted with orchards and the total area of the growing region. To allow for the possibility that some land in the growing region is used for other purposes, we allow the planted area to be a linear function of total growing region area, $L = d \times A$ where A is the total growing region area, and d ($0 < d \leq 1$) is a density parameter. This facilitates calibrating the model.

Bringing another unit of land into the growing region increases both the quantity of feedstock produced and the average distance all feedstock must be transported. The increase in feedstock quantity is linear (holding yield constant) and the increase in average delivery distance is proportional to a positive power of land, hence making the delivery cost function a convex function of growing region area.

2.6 Processing costs

Since this analysis focuses on a static, deterministic setting, the processing facility size can exactly match the level of feedstock production. Thus Q represents both the quantity of feedstock produced and the processing capacity of the facility. Nguyen and Prince (1996) and Jenkins (1997) wrote two influential studies that suggest that operating costs are a concave function of facility size. We thus write processing costs as $C_p Q^\gamma$ where $\gamma < 1$.

2.7 Objective function

Recall the manager's objective is to minimize the cost of feedstock production, given by:

$$\text{Feedstock costs} = \text{Farm gate feedstock costs} + \text{Feedstock delivery costs} + \text{Processing costs}$$

Using the notation and formulas developed in the previous section, we can rewrite the feedstock cost function mathematically

$$C(n, L) = \left[\left(C_f + \frac{C_n}{n} \right) L + C_D y(n) L^\alpha + C_P (y(n) L)^\gamma \right]$$

where n is maximum orchard age, L is area of the growing region, C_f is the age-independent cost per unit of land, C_n is the age-dependent cost per unit of land, C_D is the delivery cost parameter, α is the measure of delivery cost convexity, C_P is the processing cost parameter, and γ is the measure of processing cost concavity.

3 Cost Minimization and Comparative Statics

We now return to the manager's optimization problem, minimizing the costs of supplying a processing facility of a given size (\bar{Q}):

$$\min_{n,L} C(n, L) = \left[\left(C_f + \frac{C_n}{n} \right) L + C_D y(n) L^\alpha + C_P (y(n) L)^\gamma \right] \quad \text{s.t. } y(n)L = \bar{Q}$$

Observe that we can substitute the facility size into the expression for processing costs, leading them to become a constant relative to n and L , thereby reducing the cost minimization problem to one that only includes farm gate and delivery costs.

$$\min_{n,L} C(n, L) = \left[\left(C_f + \frac{C_n}{n} \right) L + C_D y(n) L^\alpha \right] \quad \text{s.t. } y(n)L = \bar{Q}$$

The Lagrangian associated with this cost minimization problem is

$$\mathcal{L}(n, L, \lambda) = \left(C_f + \frac{C_n}{n} \right) L + C_D y(n) L^\alpha + \lambda (\bar{Q} - y(n)L)$$

3.1 First order conditions

The three first order conditions for the cost minimization problem are

$$\frac{\partial \mathcal{L}}{\partial n} = \frac{-C_n L}{n^2} + C_D y'(n) L^\alpha - \lambda y'(n) L = 0 \quad (5)$$

$$\frac{\partial \mathcal{L}}{\partial L} = (C_f + \frac{C_n}{n}) + \alpha C_D y(n) L^{\alpha-1} - \lambda y(n) = 0 \quad (6)$$

$$\frac{\partial \mathcal{L}}{\partial \lambda} = \bar{Q} - y(n) L = 0 \quad (7)$$

Equations (5) - (7) state that the marginal change in the Lagrangian function with respect to each of the choice variables is necessarily zero at the optimum.

The left hand side of equation (5) shows how the Lagrangian function changes with respect to an increase in the orchard age. There are three components. The first component is the change in age-structure dependent costs (e.g. average replanting costs). This is always negative since the costs are averaged over more age-classes as n increases. The second component is the change in delivery costs due to the increase in orchard age. This can be either positive or negative depending on the sign of marginal yield, $y'(n)$. If marginal yield is negative, then an increase in orchard age reduces delivery costs since there is less feedstock to deliver. The third term is the penalty for violating the quantity constraint. If $y'(n)$ is non-zero, a change in n changes the quantity of feedstock produced (since we are holding planted area constant). If the constraint was satisfied before the change, then it will now be violated after the change. Generally, λ represents the penalty for violating the constraint by a single unit (at the optimum it represents the change in costs due to a unit increase in processing facility capacity). So the third term is the product of the per-unit penalty and the change in total feedstock quantity due to the increase in orchard age.

The left hand side of equation (6) shows how the Lagrangian function changes with marginal increase in the planted area. The three components have similar interpretations to the components of equation (5) except that now orchard age is being held constant. The first term is the marginal cost of growing feedstock on an additional unit of land. The second term is the marginal cost of delivery from the additional unit of land. This is an increasing function of total land due to the convexity of delivery costs. Again, the third term is the penalty for violating the capacity constraint, given the penalty per unit, λ .

3.2 Isoquant and isocost curves

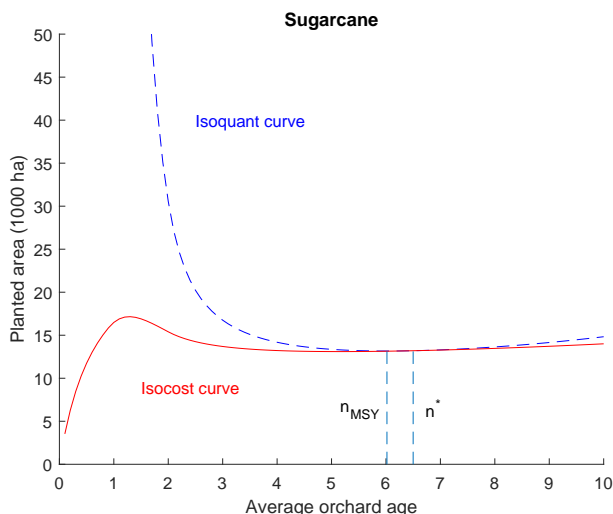


Figure 2: Example isocost and isoquant curves for the cost minimization model. In this instance, the lower contour set for the isocost curve is non-convex.

Figure 2 shows example isocost and isoquant curves for the constrained minimization problem presented in the previous section. The isocost and isoquant functions are presented in (n, L) space, so both are functions of n . The figure was generated with MATLAB using the calibration for sugarcane described in appendix B (see section 4 for more details on how this was solved numerically). Although specific to the sugarcane ethanol industry in São Paulo state, Brazil, this figure displays all the qualitative features of an isocost and isoquant curve of the general constrained minimization problem, as the next sections establish.

Looking at figure 2, two issues arise regarding using the first order conditions to solve the constrained minimization problem. The first is that the domain of the isocost and isoquant function is unbounded to the right. The second is that the lower-cost set of the isocost curve is non-convex (most obviously seen for almonds). These two issues mean that we cannot immediately invoke the usual sufficiency conditions for a convex optimization problem, which call for a bounded domain and a convex lower-contour set for the objective function and guarantee that a solution to the first order conditions is also a solution to the original optimization problem.

The first issue can be dispensed with almost immediately by noting that as n approaches infinity, yield approaches zero, requiring the growing region to increase with-

out bound. The marginal cost savings from increasing n and reducing age-independent costs approach zero as n approaches infinity, whereas the marginal cost of expanding the growing region is always positive (and in fact increasing due to the convex delivery costs). Hence it cannot be optimal to let n approach infinity, implying that for each parameter set there must be some upper bound beyond which the optimal n can never be found.

The second issue, a non-convex lower-cost set is dealt with by propositions 1–??.

3.2.1 Ruling out the optimality of $n \leq n_{MSY}$

Proposition 1 *The optimal maximum orchard age, n^* must be strictly greater than the maximum orchard age that maximizes yield, n_{MSY} , i.e. $n^* > n_{MSY}$.*

This proposition shows that production costs can never be minimized while orchard yield is an increasing function of maximum orchard age due to the presence of age-dependent costs. This is because for each $y(n)$ below the maximum, there is an n that generates an identical $y(n)$ to the left of the maximum and to the right of the maximum. The n to the right of the maximum has a lower average replanting cost, since replanting costs are dispersed over a larger number of age-classes, and thus is always the lower cost choice. The next sections establish that a solution to the first order conditions exist in the (n_{MSY}, ∞) region and that this solution also solves the cost-minimization problem. See appendix A for proof.

3.2.2 The existence of a solution to the first-order conditions

Proposition 2 *Given assumptions (1)-(4), a solution, n^* , to the first order conditions exists such that $n^* \in (n_{MSY}, \infty)$.*

The intuition behind this proof is that the derivatives of the isocost and isoquant functions must be equal somewhere on the set (n_{MSY}, ∞) . At n_{MSY} the slope of the isocost function is greater than the slope of the isoquant function. Conversely, as n approaches infinity, the slope of the isoquant approaches a positive constant while the slope of the isocost function approaches zero. By continuity there must be some intermediate point where the slopes are equal. See appendix A for proof.

3.3 The comparative statics of n^* and L^*

The signs of the comparative statics of the cost-minimization model are presented in table 1. Proofs for these signs are presented in appendix A.1. How does the optimal growing region size and maximum orchard age change as the given processing facility size changes? We answer this question by finding and analyzing the derivatives $\frac{dn^*}{dQ}$ and $\frac{dL^*}{dQ}$.

As the processing facility size increases, the optimal maximum orchard age decreases, and approaches the maximum yield age. For $n > n_{MSY}$, a decrease in n increases the yield of the feedstock growing region. Since a fixed quantity of feedstock must be produced, higher yield allows the growing region to be marginally smaller. We have shown that it is always worthwhile to marginally boost yields as the facility size increases. The magnitude of this effect, and whether it is economically important, depends on the particular parameterization of the model.

The comparative static of optimal acreage with respect to refinery size implies that when the average yield at the optimal orchard age is decreasing at an increasing rate, the land used to grow the feedstock will increase as refinery size increases. By definition, the second derivative of average yield will be negative at the maximum sustainable yield age. Therefore there is a neighborhood around n_{MSY} in which proposition ?? holds.

\mathbf{x}	$\frac{dn^*}{dx}$	$\frac{dL^*}{dx}$
Q	(< 0)	(> 0) $\Leftrightarrow y''(n^*) < 0$
C_f	(< 0)	(< 0)
C_n	(> 0)	(> 0)
C_D	(< 0)	(< 0)
α	(< 0)	(< 0) $\Leftrightarrow L > e^{-1/(\alpha-1)}$

Table 1: Signs of comparative statics of n^* and L^* .

The parameter C_f represents the age-independent cost of growing an orchard of any age. An increase in C_f increases the marginal costs of land, so the optimal choice moves away from land and toward yield through a reduction in the age.

The parameter C_n represents the age-dependent costs of the orchard. This cost includes replanting costs, as well as the cost of maintaining trees in the years after they are planted. The total cost of replanting and maintaining is dependent on the maximum orchard age, since $\frac{1}{n}$ of the orchard is being replanted and $\frac{n-1}{n}$ is being maintained each year. See appendix B for more details. An increase in positive age-dependent costs always increases the attractiveness of older trees, since older trees are relatively cheaper than new trees.

The parameter C_D represents the costs of delivering feedstock from the field to the processing facility. It affects both costs of yield and of land, since both these variables determine the quantity of feedstock transported. However, since this analysis is focused on a cost-minimization problem with respect to a fixed facility size, a change in delivery cost only affects the marginal cost of land, leaving the quantity of feedstock produced unchanged. Therefore, an increase in the delivery cost increases the marginal cost of land, and like the effect of C_f , shifts the optimal mixture of land and yield towards yield and away from land.

4 Simulations for numerical comparative statics

Figure 3 shows a numerical example of how the cost minimizing orchard age and planted land area change as the processing facility processing capacity is increased. The example is calibrated to sugarcane mills in São Paulo state, which range from 1 million to 36 million tons per year. The details of the calibration are provided in appendix B.1.

The shape of the expansion path corresponds to the results of the comparative statics of n^* and L^* as we increase \bar{Q} . As mill capacity increases from 1 to 36 million tons the optimal maximum orchard age decreases from 6.50 to 6.21, corresponding to an increase in the n -orchard yield from 75.76 tons per hectare to 75.92 tons per hectare. The majority of the additional feedstock is supplied from additions to planted land area.

Figure 4 shows the difference in cost between the cost of choosing both n and L to minimize the cost of supplying the processing facility and the cost of fixing n at n_{MSY} and only allowing L to vary. For sugarcane, the cost difference when supplying a one million ton facility (the smallest reported in Crago et al. (2010)) is 0.21 percent. This cost difference is small at 0.25 percent.

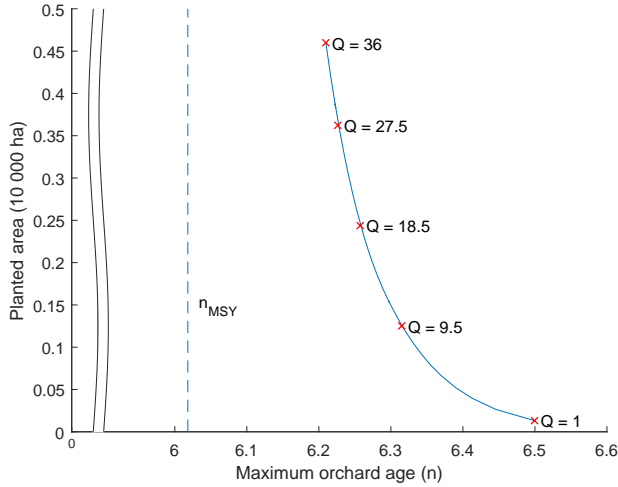


Figure 3: Cost minimizing age and planted land area as processing facility capacity is increased from 1 million tons to 36 million tons. With increased capacity, age approaches n_{MSY} ($= 5.31$).

As the processing facility’s capacity increases, the difference in cost decreases, asymptotically approaching zero. For the range of facilities presented in the graph, the condition for the comparative static of land with respect to refinery capacity is satisfied and the increased capacity is met with an increase in land and a decrease in optimal age toward n_{MSY} .

Given the small magnitude of the percentage cost reductions, a natural question arises: how robust is this result? Does this particular parameter set lead to an unusually small cost reduction, or are the cost reductions relative to MSY likely to be small for all vertically integrated sugarcane mills with parameters in the neighborhood of the baseline calibration?

To test this question, we performed a Monte Carlo simulation with parameters drawn from a uniform distribution generated by scaling draws from a Halton sequence. For cost parameters, we centered the uniform distribution on the calibrated parameter values, with a minimum parameter value of half the calibrated value, and a maximum value of 1.5 times the calibrated value. Mill capacity ranged between 1 and 37 million tons (the range from Crago et al. (2010)). The parameter values used in the simulation

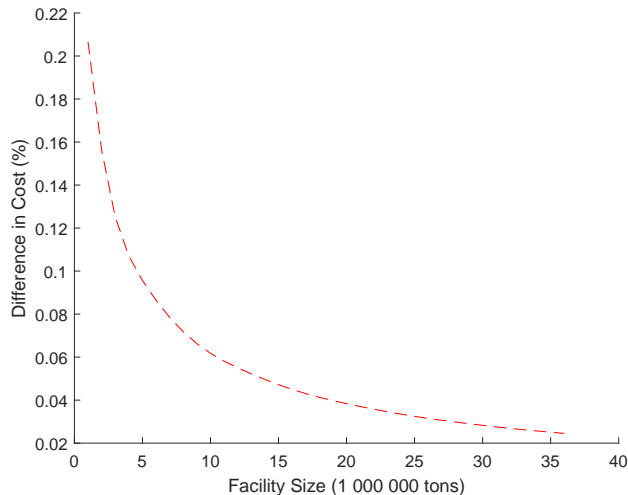


Figure 4: Percentage difference in cost between using the cost-minimizing and maximum sustainable yield ages for the range of processing facility sizes present in Brazil.

are reported in table 3 in appendix B.2. The processing facility size was not varied. Using MATLAB, we generated 100 000 random parameter sets. For each random parameter set, the `fmincon` function was used to solve for the cost minimizing values of n and L along with the associated costs for feeding the facility using the minimized and MSY ages. Because of numerical issues or theoretical incompatibility, 15 936 draws were eliminated.

The results of the simulations from random parameter draws are shown as an empirical cumulative density function in figure 5. The distribution is truncated at zero—optimizing the age of the orchard should never *increase* costs. The simulated cost reductions are right skewed. The cost difference for the original calibrated value is roughly centered in the simulated data, located at the 51.4th percentile. Despite the long tail, 99 percent of simulated results have a percentage cost difference less than 1.42 percent.

The simulations allow us to construct numerical comparative statics for all parameters, using linear regression on the simulated data. The results of these regressions are shown in table 2. Each column is a regression of either total cost, optimal age, or optimal land on the parameters and a constant. The natural logarithm of all dependent and independent variables has been taken, so estimated coefficients should be

	$\ln(Cost)$	$\ln(n^*)$	$\ln(L^*)$
$\ln(t_1)$	0.042* (0.003)	0.111* (0.000)	0.064* (0.000)
$\ln(t_{max})$	0.021 (0.007)	0.355* (0.001)	0.055* (0.000)
$\ln(t_T)$	-0.166* (0.014)	0.397* (0.001)	-0.176* (0.001)
$\ln(f_{max})$	-0.821* (0.010)	-0.003* (0.001)	-1.000* (0.000)
$\ln(C_D)$	0.502* (0.010)	-0.005* (0.001)	-0.000 (0.000)
$\ln(C_n)$	0.053* (0.010)	0.030* (0.001)	0.002* (0.000)
$\ln(C_f)$	0.451* (0.010)	-0.028* (0.001)	-0.002* (0.000)
$\ln(\alpha)$	10.030* (0.016)	-0.145* (0.001)	-0.007* (0.001)
$\ln(Q)$	1.318* (0.004)	-0.002* (0.000)	1.000* (0.000)
Intercept	Yes	Yes	Yes
Adj. R ²	0.853	0.907	0.998
Num. obs.	84064	84064	84064
F statistic	54414.186	91157.246	5558060.818

* $p < 0.001$

Table 2: Numerical comparative statics. Linear regression of total cost, optimal age, and optimal land on all parameters.

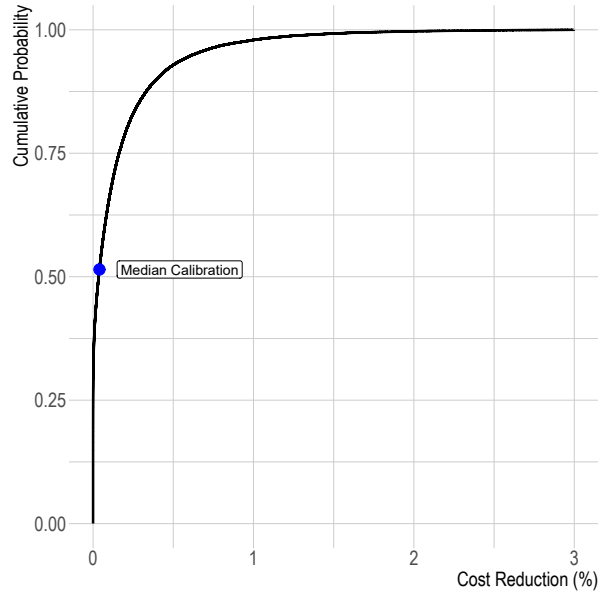


Figure 5: Empirical cumulative density functions of percentage cost reduction for sugarcane Monte Carlo simulations

interpreted as elasticities.

The signs of the coefficients are consistent with the theoretical signs presented in table 1, with the exception of the effect of delivery cost on land area. This coefficient is not statistically different from zero. Given the parameter values, an increase in delivery costs by one percent increases total costs by 0.5 percent, with a marginal reduction in age and no appreciable change in land.

For the age-yield function, increases in the age of at first yield, age of maximum yield, and age of final yield all increase the optimal age, while increase in the maximum yield decrease the optimal age.

5 Discussion

The optimal orchard age is very close to the yield-maximizing orchard age in the vast majority of simulations. From the comparative statics in table 1 we know that increases in age-structure independent costs, delivery costs, and delivery cost convexity all decrease the optimal orchard age. We can infer that in the examples these three costs dominate the age-structure dependent costs. This is supported by the numerical

comparative statics. Each of these three parameters has relatively large coefficients.

A surprising result from the model is that smaller processing facilities have proportionally larger cost savings. One might think, *a priori*, that the cost savings would be larger for larger refineries because they require more feedstock, so lowering the cost of feedstock would be more beneficial. However, it is because larger refineries require large quantities, thereby incurring high marginal delivery costs due to the greater extent of the growing region and making the age-structure dependent costs relatively small, that they are least benefited by optimizing age.

Focusing on cost-minimization hides a potential channel for age optimization to affect the management of the growing-processing operation. By keeping the processing facility size fixed, a change in a parameter only causes a substitution between land and age. In a more flexible model that also optimized the facility capacity choice, the same parameter change would have two effects: the substitution effect from the change in the relative cost of land and age; and the size effect, where the change in the parameter alters the optimal size of the facility. These two effects may reinforce or offset each other. For example, the effects may offset when a decrease in delivery costs increases the optimal age through the substitution effect (land is relatively cheaper), and also increase the optimal size of the facility, which would reduce the optimal age. This example is based on the comparative statics in section 3.3, but a simultaneous analysis of both the substitution and size effects would require a net present value maximization model with endogenous processing facility capacity choice.

Furthermore, the current model requires that feedstock production exactly match processing facility capacity. This can be thought of as a long-run situation where the facility has been optimized for the downstream market and the growing region has been optimized for the facility. However, in reality, managers can run the facility below capacity in the short run, or sell excess feedstock to other processors (assuming delivery costs are not prohibitive). We assume that these short-term fluctuations are smoothed out in this model.

This long-run assumption also ignores the problem of achieving the optimal age in a least-cost method. Margarido and Santos (2012) present a sugarcane planting sequence for feeding a 2 000 000 ton facility. This sequence front loads the planting in the first three years of production and plants the equilibrium area each following year, resulting in a stable age nine years after the initial planting. Although the authors note that the initial front loading is necessary because the facility needs to crush a

larger amount of sugarcane in the first year, there is no discussion of the optimality of this planting sequence, or comparisons with alternative sequences. Therefore, the cost-minimizing age from this model should be considered a long-run average target, with year-to-year fluctuations around the target. The details of achieving the target should be determined for the particular application.

6 Conclusion

We have, to our knowledge, presented the first model of optimal perennial crop age when the output is used as a feedstock for a processing facility of a given size. To account for non-convexities in the cost-minimization problem, we proved under certain assumptions on the age-yield function, that the first order conditions of the model have a solution. We generated analytical and numeric comparative statics of this solution with respect to facility size and cost parameters. We also provided a simulation calibrated to the sugarcane industry in São Paulo, Brazil.

From the results we can conclude that it is indeed possible to reduce biorefinery feedstock costs by optimizing the feedstock age, but in the case of the São Paulo sugarcane industry, the benefits are small relative to the reference case of the yield-maximizing age.

The importance of age-structure optimization for managers must be considered on a case-by-case basis, depending on whether the parameters of the particular problem generate a large cost saving from optimization, or whether the yield-maximizing age is a good heuristic. Further, if the orchard is currently managed at some age other than the yield-maximizing age, this alternative age must be used as a reference, possibly generating still greater cost savings.

References

- Alexander, C., R. Ivanic, S. Rosch, W. Tyner, S.Y. Wu, and J.R. Yoder. 2012. “Contract theory and implications for perennial energy crop contracting.” *Energy Economics* 34:970–979.
- Barrett, C.B., T. Reardon, J. Swinnen, and D. Zilberman. Forthcoming. “Agri-Food Value Chain Revolutions in Low- and Middle-Income Countries.” *Journal of Economic Literature*, pp. .

- Crago, C.L., M. Khanna, J. Barton, E. Giuliani, and W. Amaral. 2010. “Competitiveness of Brazilian sugarcane ethanol compared to US corn ethanol.” *Energy Policy* 38:7404–7415.
- De Meyer, A., D. Cattrysse, J. Rasinmäki, and J. Van Orshoven. 2014. “Methods to optimise the design and management of biomass-for-bioenergy supply chains: A review.” *Renewable and Sustainable Energy Reviews* 31:657–670.
- Debnath, D., F.M. Epplin, and A.L. Stoecker. 2014. “Managing Spatial and Temporal Switchgrass Biomass Yield Variability.” *Bioenergy Research* 7:946–957.
- . 2015. “Switchgrass procurement strategies for managing yield variability: Estimating the cost-efficient D (downtime cost) L (land to lease) frontier.” *Biomass and Bioenergy* 77:110–122.
- Douglas, J., J. Lemunyon, R. Wynia, and P. Salon. 2009. “Planting and Managing Switchgrass as a Biomass Energy Crop.” Working paper No. 3, United States Department of Agriculture, Natural Resources Conservation Service, Plant Materials Program, Sep.
- Du, X., L. Lu, T. Reardon, and D. Zilberman. 2016. “Economics of Agricultural Supply Chain Design: A Portfolio Selection Approach.” *American Journal of Agricultural Economics* 98:1377–1388.
- Glover, J.D., J.P. Reganold, L.W. Bell, J. Borevitz, E.C. Brummer, E.S. Buckler, C.M. Cox, T.S. Cox, T.E. Crews, S.W. Culman, L.R. DeHaan, D. Eriksson, B.S. Gill, J. Holland, F. Hu, B.S. Hulke, A.M.H. Ibrahim, W. Jackson, S.S. Jones, S.C. Murray, A.H. Paterson, E. Ploschuk, E.J. Sacks, S. Snapp, D. Tao, D.L. Van Tassel, L.J. Wade, D.L. Wyse, and Y. Xu. 2010. “Increased Food and Ecosystem Security via Perennial Grains.” *Science* 328:1638–1639.
- Heaton, E. 2010. “Giant Miscanthus for Biomass Production.” Working paper, Iowa State University Extension.
- Hochman, G., and D. Zilberman. 2018. “Corn Ethanol and U.S. Biofuel Policy 10 Years Later: A Quantitative Assessment.” *American Journal of Agricultural Economics* 100:570–584.

- Jenkins, B.M. 1997. “A comment on the optimal sizing of a biomass utilization facility under constant and variable cost scaling.” *Biomass and Bioenergy* 13:1–9.
- Khanna, M., and C.L. Crago. 2012. “Measuring Indirect Land Use Change with Biofuels: Implications for Policy.” *Annual Review of Resource Economics* 4:161–184.
- Kreitzman, M., E. Toensmeier, K.M.A. Chan, S. Smukler, and N. Ramankutty. 2020. “Perennial Staple Crops: Yields, Distribution, and Nutrition in the Global Food System.” *Frontiers in Sustainable Food Systems* 0.
- Mafakheri, F., and F. Nasiri. 2014. “Modeling of biomass-to-energy supply chain operations: Applications, challenges and research directions.” *Energy Policy* 67:116–126.
- Malladi, K.T., and T. Sowlati. 2018. “Biomass Logistics: A Review of Important Features, Optimization Modeling and the New Trends.” *Renewable and Sustainable Energy Reviews* 94:587–599.
- Manochio, C., B. Andrade, R. Rodriguez, and B. Moraes. 2017. “Ethanol from Biomass: A Comparative Overview.” *Renewable and Sustainable Energy Reviews* 80:743–755.
- Margarido, F.B., and F. Santos. 2012. “Agricultural Planning.” In F. Santos, A. Borém, and C. Caldas, eds. *Sugarcane Bioenergy, Sugar and Ethanol – Technology and Prospects*. Ministry of Agriculture, Livestock and Food Supply, chap. 1, pp. 7–21.
- McCarty, T., and J. Sesmero. 2021. “Contracting for Perennial Energy Crops and the Cost-Effectiveness of the Biomass Crop Assistance Program.” *Energy Policy* 149:112018.
- Mitra, T., D. Ray, and R. Roy. 1991. “The economics of orchards: an exercise in point-input, flow-output capital theory.” *Journal of Economic Theory* 53:12–50.
- Molnar, T., P. Kahn, T. Ford, C. Funk, and C. Funk. 2013. “Tree Crops, a Permanent Agriculture: Concepts from the Past for a Sustainable Future.” *Resources* 2:457–488.
- Nguyen, M.H., and R.G.H. Prince. 1996. “A simple rule for bioenergy conversion plant size optimisation: Bioethanol from sugar cane and sweet sorghum.” *Biomass and Bioenergy* 10:361–365.

- O'Neill, E.G., and C.T. Maravelias. 2021. "Towards Integrated Landscape Design and Biofuel Supply Chain Optimization." *Current Opinion in Chemical Engineering* 31:100666.
- Overend, R.P. 1982. "The average haul distance and transportation work factors for biomass delivered to a central plant." *Biomass* 2:75–79.
- Rentizelas, A.A., A.J. Tolis, and I.P. Tatsiopoulos. 2009. "Logistics issues of biomass: The storage problem and the multi-biomass supply chain." *Renewable and Sustainable Energy Reviews* 13:887–894.
- Riley, F.R. 2002. "Olive Oil Production on Bronze Age Crete: Nutritional Properties, Processing Methods and Storage Life of Minoan Olive Oil." *Oxford Journal of Archaeology* 21:63–75.
- Sant'Anna, A.C., J.S. Bergtold, A. Shanoyan, G. Granco, and M.M. Caldas. 2018. "Examining the Relationship between Vertical Coordination Strategies and Technical Efficiency: Evidence from the Brazilian Ethanol Industry." *Agribusiness* 34:793–812.
- Sharma, B., R.G. Ingalls, C.L. Jones, and A. Khanchi. 2013. "Biomass supply chain design and analysis: Basis, overview, modeling, challenges, and future." *Renewable and Sustainable Energy Reviews* 24:608–627.
- Teixeira, F.L.D.S. 2013. "Custo Médio Operacional da Lavoura de Cana-de-açúcar em Reais."
- Tisdell, C.A., and N.T.M.H. De Silva. 1986. "Supply-Maximising and Variation-Minimizing Replacement Cycles of Perennial Crops and Similar Assets: Theory Illustrated by Coconut Cultivation." *Agricultural Economics* 37:243–251.
- Wallace, J. 2000. "Increasing agricultural water use efficiency to meet future food production." *Agriculture, Ecosystems & Environment* 82:105–119.
- Wang, R. 2007. "The Optimal Consumption and the Quitting of Harmful Addictive Goods." *The B.E. Journal of Economic Analysis & Policy* 7.
- Wright, M., and R.C. Brown. 2007. "Establishing the optimal sizes of different kinds of biorefineries." *Biofuels, Bioproducts and Biorefining* 1:191–200.

Zahraee, S.M., N. Shiwakoti, and P. Stasinopoulos. 2020. “Biomass Supply Chain Environmental and Socio-Economic Analysis: 40-Years Comprehensive Review of Methods, Decision Issues, Sustainability Challenges, and the Way Forward.” *Biomass and Bioenergy* 142:105777.

Zilberman, D., L. Lu, and T. Reardon. 2019. “Innovation-Induced Food Supply Chain Design.” *Food Policy* 83:289–297.

A Proofs of Propositions and Lemmas

Lemma 1 *The optimal maximum orchard age must be greater than or equal to the maximum yield age, i.e. $n^* \geq n_{MSY}$.*

Proof of Lemma 1.

From our assumptions on the age-yield function in section 2.1.2, for all yields less than the maximum yield, there are two orchard ages that generate that yield. That is, for all $\bar{y} \in (0, y(n_{MSY}))$, there exist $n_{\bar{y}}^- < n_{MSY} < n_{\bar{y}}^+$, such that $y(n_{\bar{y}}^-) = y(n_{\bar{y}}^+) = \bar{y}$.

On the graph of the isoquant, these two n values generate the same area, \bar{L} , since $L = \frac{\bar{Q}}{y(n)}$ so $\frac{\bar{Q}}{y(n_{\bar{y}}^-)} = \frac{\bar{Q}}{y(n_{\bar{y}}^+)} = \bar{L}$.

Now compare the costs of these two n values.

$$\begin{aligned} C(n_{\bar{y}}^-, \bar{L}) - C(n_{\bar{y}}^+, \bar{L}) &= \left(C_f + \frac{C_n}{n_{\bar{y}}^-} \right) \bar{L} + C_D y(n_{\bar{y}}^-) \bar{L}^\alpha - \left(C_f + \frac{C_n}{n_{\bar{y}}^+} \right) \bar{L} - C_D y(n_{\bar{y}}^+) \bar{L}^\alpha \\ &= \left(C_f + \frac{C_n}{n_{\bar{y}}^-} \right) \bar{L} + C_D \bar{y} \bar{L}^\alpha - \left(C_f + \frac{C_n}{n_{\bar{y}}^+} \right) \bar{L} - C_D \bar{y} \bar{L}^\alpha \\ &= C_n \bar{L} \left(\frac{1}{n_{\bar{y}}^-} - \frac{1}{n_{\bar{y}}^+} \right) (> 0) \end{aligned}$$

Hence for any level of yield, the cost minimizing maximum orchard age is greater than or equal to the maximum yield age, i.e. $n^* \geq n_{MSY}$. ■

Lemma 2 *The minimum of the isoquant is located at n_{MSY} .*

Proof of Lemma 2.

The isoquant is defined by $y(n)L = \bar{Q}$. This can be rewritten so that L is a function of n , i.e. for a particular level of feedstock production $L = \frac{\bar{Q}}{y(n)}$. The minimum of

this function (i.e. the least quantity of land necessary to produce the desired quantity) occurs when the derivative of this function is set to zero.

$$\left. \frac{dL}{dn} \right|_{\text{isoquant}} = \frac{-\bar{Q}y'(n)}{[y(n)]^2} = 0 \Leftrightarrow y'(n) = 0$$

From the conditions imposed on the age-yield function in section 2.1.2 there is a unique maximum of the yield function located at n_{MSY} . Hence the unique minimum of the isoquant function occurs at n_{MSY} . ■

Lemma 3 *The minimum of the isocost curve is located at $n < n_{MSY}$.*

Proof of Lemma 3.

The isocost curve is defined by a level set of the cost function: $C(n, L) = \bar{C}$. We wish to locate the set of local extrema of the isocost curve, where L is expressed as a function of n . This set is a subset of the critical points of $\frac{dL}{dn}$.

Totally differentiate the cost function:

$$\left[\left(C_f + \frac{C_n}{n} \right) + \alpha C_D y(n) L^{\alpha-1} \right] dL + \left[\frac{-C_n L}{n^2} + C_D y'(n) L^\alpha \right] dn = 0$$

Thus

$$\left. \frac{dL}{dn} \right|_{\text{isocost}} = \frac{C_n L/n^2 - C_D y'(n) L^\alpha}{\left(C_f + \frac{C_n}{n} \right) + \alpha C_D y(n) L^{\alpha-1}} = 0 \Leftrightarrow C_n L/n^2 = C_D y'(n) L^\alpha$$

since all the terms in the denominator are non-negative. The only term in this last equality that can change sign is $y'(n)$. All other terms are constrained to be non-negative. Hence the equality cannot be satisfied if $y'(n) < 0$, which occurs when $n > n_{MSY}$. Also, if $n = n_{MSY}$ it must be that $L = 0$ for the equality to be satisfied. If $L = 0$ we have $C(n_{MSY}, 0) = 0$, so for any positive level of cost $(n_{MSY}, 0)$ is not an element of the graph of the isocost function, and n_{MSY} cannot be a critical point. Hence for any positive level of cost, any extrema of the isocost function must occur when $n < n_{MSY}$. ■

Lemma 4 *The isocost curve has a positive slope for all $n \geq n_{MSY}$.*

Proof of Lemma 4.

This follows immediately from the proof of lemma 3 since the expression for the slope

of the isoquant curve is strictly positive for all $n > n_{MSY}$. ■

Proof of proposition 1.

The optimal n must be strictly greater than n_{MSY} , i.e. $n^* > n_{MSY}$.

The isocost curve has a positive slope for all $n \geq n_{MSY}$ (lemma 4). The isoquant curve has a zero slope at n_{MSY} (lemma 2). Hence the isocost and isoquant curves cannot be tangential at n_{MSY} , so $n^* \neq n_{MSY}$. Combining this with lemma 1 gives us the result.

■

Lemma 5 Assumptions (1)-(4) imply that $0 < \lim_{n \rightarrow \infty} \int_0^n f(a) da < \infty$

Proof of Lemma 5.

We can split $\lim_{n \rightarrow \infty} \int_0^n f(a) da$ in two by partitioning its domain:

$$\begin{aligned} \lim_{n \rightarrow \infty} \int_0^n f(a) da &= \lim_{n \rightarrow \infty} \int_0^k f(a) da + \lim_{n \rightarrow \infty} \int_k^n f(a) da \\ &= \int_0^k f(a) da + \lim_{n \rightarrow \infty} \int_k^n f(a) da \end{aligned}$$

Now consider $\int_0^k f(a) da$. The age-yield function is bounded below by 0 by construction ($f(a)$ represents a physical quantity). Assumptions (1)-(3) imply that $f(a)$ is bounded above. Hence $f(a)$ is bounded on the domain $[0, k]$ for all $k \in \mathbb{R}_{>0}$. Thus $0 \leq \int_0^k f(a) da < \infty$ since this is the integral of a bounded positive function on a finite domain.

We must consider two possibilities when analyzing $\lim_{n \rightarrow \infty} \int_k^n f(a) da$: either $f(a) > 0$ for all $a \in \mathbb{R}_{\geq 0}$, or there exists some $\hat{k} \in \mathbb{R}_{\geq 0}$ such that for all $a > \hat{k}$ $f(a) = 0$. In the first case, we must establish that $\lim_{n \rightarrow \infty} \int_k^n f(a) da$ approaches zero fast enough that $\lim_{n \rightarrow \infty} \int_k^n f(a) da$ is not infinite. Assumption (4) implies that there exist $k \in \mathbb{R}_{\geq 0}$ and $p > 1$ such that for all $a > k$ $f(a) < \frac{1}{a^p}$ (if such k and p did not exist, $\lim_{n \rightarrow \infty} \int_k^n f(a) da$ would either be strictly positive, or infinite). Thus

$$\lim_{n \rightarrow \infty} \int_k^n f(a) da < \lim_{n \rightarrow \infty} \int_k^n \frac{1}{a^p} da < \infty$$

since integrals of the form $\int_k^\infty \frac{1}{x^p} dx$ are convergent if and only if $p > 1$. In the second case, $\lim_{n \rightarrow \infty} \int_k^n f(a) da = 0$, and $\lim_{n \rightarrow \infty} \int_0^n f(a) da = \int_0^{\hat{k}} f(a) da$. Thus $0 \leq \lim_{n \rightarrow \infty} \int_0^n f(a) da < \infty$

Assumption 3 implies that $f(a)$ is strictly positive on some subset of $\mathbb{R}_{\geq 0}$ with non-empty interior. Hence $\lim_{n \rightarrow \infty} \int_0^n f(a) da > 0$

Therefore $0 < \lim_{n \rightarrow \infty} \int_0^n f(a) da < \infty$ ■

Proof of proposition 2.

Given assumptions (1)-(4), a solution, n^* , to the cost minimization problem exists such that $n^* \in (n_{MSY}, \infty)$.

Sketch of the proof: We have already demonstrated that n^* must be greater than n_{MSY} . At n_{MSY} the slope of the isocost curve is strictly positive and the slope of the isoquant curve is zero. We show that as n approaches infinity, the slope of the isocost curve approaches zero, while the slope of the isoquant curve approaches a positive value. By continuity the slope functions must cross at least once, and hence there must exist at least one point where the isocost and isoquant curves are tangent to each other.

We begin by showing that the slope of the isocost curve approaches zero as n approaches infinity. The slope of the isocost function when L is written as a function of n (as derived in lemma 2)

$$\left. \frac{dL}{dn} \right|_{\text{isocost}} = \frac{C_n L(n)/n^2 - C_D y'(n) L(n)^\alpha}{(C_f + \frac{C_n}{n}) + \alpha C_D y(n) L(n)^{\alpha-1}}$$

To take the limit of this expression as n approaches infinity, we need to know how $L(n)$ on the isocost function behaves as n approaches infinity. The isocost function is defined as

$$C(n, L) = (C_f + \frac{C_n}{n})L + C_D y(n) L^\alpha = \bar{C}$$

This implicitly defines L as a function of n .

$$C(n) = (C_f + \frac{C_n}{n})L(n) + C_D y(n) L(n)^\alpha = \bar{C}$$

Now we take the limit of this expression as $n \rightarrow \infty$ and solve for the unknown value

L_∞ .

$$\begin{aligned} \lim_{n \rightarrow \infty} (C_f + \frac{C_n}{n})L(n) + C_D y(n) L(n)^\alpha &= \bar{C} \\ \Rightarrow C_f L_\infty &= \bar{C} \\ \Rightarrow L_\infty &= \frac{\bar{C}}{C_f} \quad \text{A constant} \end{aligned}$$

Returning to the derivative of the isocost function

$$\begin{aligned} \lim_{n \rightarrow \infty} \frac{dL}{dn} \Big|_{\text{isocost}} &= \lim_{n \rightarrow \infty} \frac{C_n L(n)/n^2 - C_D y'(n) L^\alpha}{(C_f + \frac{C_n}{n}) + \alpha C_D y(n) L(n)^{\alpha-1}} \\ &= \frac{0 - 0}{C_f + 0 + 0} \quad \begin{array}{l} \text{Since } y(n) \text{ and } y'(n) \text{ both approach } 0, \\ \text{and } L(n) \text{ approaches a constant as } n \rightarrow \infty \end{array} \\ &= 0 \end{aligned}$$

Now we show that under a certain condition the slope of the isoquant function approaches a positive constant as $n \rightarrow \infty$. The isoquant function is given by $y(n) L = \bar{Q}$ and can be rewritten as

$$\begin{aligned} L &= \frac{\bar{Q}}{\frac{1}{n} \int_0^n f(a) da} \\ &= \frac{\bar{Q} n}{\int_0^n f(a) da} \end{aligned}$$

The slope of the isoquant function is given by

$$\frac{dL}{dn} \Big|_{\text{isoquant}} = \frac{\bar{Q} (\int_0^n f(a) da - n f(n))}{[\int_0^n f(a) da]^2}$$

The limit of the slope as n approaches infinity is

$$\begin{aligned}
\lim_{n \rightarrow \infty} \frac{dL}{dn} \Big|_{\text{isoquant}} &= \lim_{n \rightarrow \infty} \frac{\bar{Q} \left(\int_0^n f(a) da - n f(n) \right)}{\left[\int_0^n f(a) da \right]^2} \\
&= \bar{Q} \frac{\lim_{n \rightarrow \infty} \left(\int_0^n f(a) da - n f(n) \right)}{\lim_{n \rightarrow \infty} \left[\int_0^n f(a) da \right]^2} && \text{since } \lim_{n \rightarrow \infty} \int_0^n f(a) da > 0 \\
&&& \text{(Lemma 5)} \\
&&& \text{since} \\
&&& \lim_{n \rightarrow \infty} \int_0^n f(a) da \\
&&& > n f(n) = 0 \\
&&& \text{and} \\
&&& 0 < \lim_{n \rightarrow \infty} \int_0^n f(a) da < \infty \\
&&& \text{(Lemma 5)} \\
&= \bar{Q} \frac{\overbrace{\lim_{n \rightarrow \infty} \int_0^n f(a) da}^+ - \lim_{n \rightarrow \infty} n f(n)}{\underbrace{\lim_{n \rightarrow \infty} \left[\int_0^n f(a) da \right]^2}_+} \\
&\implies 0 < \lim_{n \rightarrow \infty} \frac{dL}{dn} \Big|_{\text{isoquant}} < \infty
\end{aligned}$$

Now define a function that returns the difference in the slopes of the isocost and isoquant functions, $h(n) = \frac{dL}{dn} \Big|_{\text{isocost}} - \frac{dL}{dn} \Big|_{\text{isoquant}}$. Since both constituent functions are continuous on the interval (n_{MSY}, ∞) , $h(n)$ is also continuous on this interval. At the maximum yield age $h(n_{MSY}) > 0$ (from lemmas 2 and 4) and, as we have just shown, when n approaches infinity the limit of $h(n)$ is strictly less than zero. Hence by the intermediate value theorem, there must exist some $n^* \in (n_{MSY}, \infty)$ such that $h(n) = 0$, and the isocost and isoquant curves are tangent to one another. ■

A.1 Proofs of comparative static results

Proof of $\frac{dn^*}{dQ} < 0$.

As processing facility size increases, the optimal orchard age decreases, i.e. $\frac{dn^}{dQ} < 0$.*

Totally differentiating $g(n, \bar{Q})$ (The derivative of the cost function when the constraint is used to eliminate L — derived in the proof of proposition 2) gives us an expression for the desired comparative static

$$\frac{dn^*}{d\bar{Q}} = \frac{-g_{\bar{Q}}}{g_n}$$

At an optimum the second order condition for a minimum must hold, so g_n must be positive. Hence

$$\text{sign}\left(\frac{dn^*}{d\bar{Q}}\right) = -\text{sign}(g_{\bar{Q}})$$

Differentiating $g(n, \bar{Q})$ with respect to \bar{Q} , and evaluating at the optimum yields

$$g_{\bar{Q}} = -(1 - \alpha)^2 \underbrace{[y(n^*)]^{-\alpha}}_{+} \underbrace{y'(n^*)}_{-} \underbrace{\bar{Q}^{\alpha-2}}_{+} \quad (> 0)$$

Hence

$$\frac{dn^*}{d\bar{Q}} < 0$$

■

Proof of $\frac{dn^*}{d\bar{Q}} > 0 \Leftrightarrow y''(n^*) < 0$.

The change in optimal growing region size with respect to a change in processing facility capacity is generally ambiguous, but if $y''(n^) < 0$, then increased processing facility capacity leads to increase growing region size, i.e. $\frac{dL^*}{d\bar{Q}} > 0$.*

To analyze this comparative static of the constrained cost minimization problem using the substitution method we need to define the inverse yield function, $g(y) = n$ ($g^{-1}(n) = y(n)$). Since the yield function is not surjective, we can only define and analyze the inverse yield on a subset of the domain. Fortunately, as shown by proposition 1, the optimal n is found in the subset $n > n_{MSY}$. On this subset the yield function is bijective, and we are guaranteed the existence of $g(y)$.

Using the constraint on processing facility capacity ($y(n)L = \bar{Q} \Rightarrow y(n) = \frac{\bar{Q}}{L}$ and $n = g\left(\frac{\bar{Q}}{L}\right)$) we can rewrite the cost function as a function of growing region only.

$$C(n(L), L) = \left(C_f + \frac{C_n}{g\left(\frac{\bar{Q}}{L}\right)} \right) L + C_D \bar{Q} L^{\alpha-1}$$

The first order condition with respect to a minimum is

$$\frac{dC}{dL} = C_f + \frac{C_n}{g\left(\frac{\bar{Q}}{L}\right)} + \frac{\bar{Q} C_n g'\left(\frac{\bar{Q}}{L}\right)}{L \left[g\left(\frac{\bar{Q}}{L}\right)\right]^2} + (\alpha - 1)C_D \bar{Q} L^{\alpha-2} = 0$$

Cross multiply by $L \left[g\left(\frac{\bar{Q}}{L}\right)\right]^2$

$$h(L) = C_f L \left[g\left(\frac{\bar{Q}}{L}\right)\right]^2 + C_n L g\left(\frac{\bar{Q}}{L}\right) + C_n \bar{Q} g'\left(\frac{\bar{Q}}{L}\right) + (\alpha - 1)C_D \bar{Q} \left[g\left(\frac{\bar{Q}}{L}\right)\right]^2 L^{\alpha-1} = 0$$

Totally differentiating $h(n, \bar{Q})$ gives us an expression for the desired comparative static

$$\frac{dL^*}{d\bar{Q}} = \frac{-h_{\bar{Q}}}{h_L}$$

At an optimum the second order condition for a minimum must hold, so g_n must be positive. Hence

$$\text{sign}\left(\frac{dL^*}{d\bar{Q}}\right) = -\text{sign}(h_{\bar{Q}})$$

$$h_{\bar{Q}} = (\alpha - 1)C_D \left[g\left(\frac{\bar{Q}}{L}\right)\right]^2 L^{\alpha-1} \quad (>) \quad (8)$$

$$+ 2(\alpha - 1)C_D \bar{Q} g\left(\frac{\bar{Q}}{L}\right) g'\left(\frac{\bar{Q}}{L}\right) L^{\alpha-2} \quad (<) \quad (9)$$

$$+ 2C_f g\left(\frac{\bar{Q}}{L}\right) g'\left(\frac{\bar{Q}}{L}\right) \quad (<) \quad (10)$$

$$+ 2C_n g'\left(\frac{\bar{Q}}{L}\right) \quad (<) \quad (11)$$

$$+ \frac{C_n \bar{Q} g''\left(\frac{\bar{Q}}{L}\right)}{L} \quad (\text{Ambiguous}) \quad (12)$$

If $g''\left(\frac{\bar{Q}}{L}\right) < 0$ at L^* , the term 12 in $h_{\bar{Q}}$ is negative.

Aside: Rewriting this condition in terms of $y(n^*)$

This condition on the second derivative of the inverse yield function is not particularly intuitive. We can rewrite this condition in terms of $y(n^*)$ which makes it much easier to understand. To do this we must rewrite this condition on the second derivative of an inverse function in terms of the original function. The relationship between the second derivative of a function and its inverse is

$$(f^{-1})''(f(x)) = \frac{-f''(x)}{[f'(x)]^3}$$

For the inverse yield function this becomes

$$g''\left(\frac{\bar{Q}}{L}\right) = g''(y(n^*)) = \frac{-y''(n^*)}{[y'(n^*)]^3}$$

So

$$g''\left(\frac{\bar{Q}}{L}\right) < 0 \Leftrightarrow \frac{-y''(n^*)}{[y'(n^*)]^3} < 0$$

Since $y'(n^*) < 0$ and the cubing operation preserves sign, this inequality is satisfied if and only if $y''(n^*) < 0$.

Returning to the proof

Given that $y''(n^*) < 0$, we now show that term (8) plus term (9) is negative.

$$(8) + (9) = (\alpha - 1)C_D \left[g\left(\frac{\bar{Q}}{L}\right) \right]^2 L^{\alpha-1} + 2(\alpha - 1)C_D \bar{Q} g\left(\frac{\bar{Q}}{L}\right) g'\left(\frac{\bar{Q}}{L}\right) L^{\alpha-2}$$

Extract common factors

$$(8) + (9) = \underbrace{(\alpha - 1)C_D g\left(\frac{\bar{Q}}{L}\right) L^{\alpha-1}}_{>0} \left[g\left(\frac{\bar{Q}}{L}\right) + 2\bar{Q} g'\left(\frac{\bar{Q}}{L}\right) L^{-1} \right]$$

Therefore

$$\text{sign}((8) + (9)) = \text{sign} \left(g\left(\frac{\bar{Q}}{L}\right) + 2\bar{Q} g'\left(\frac{\bar{Q}}{L}\right) L^{-1} \right)$$

Substitute the definition of $\bar{Q} = y(n) L$

$$\begin{aligned}
& g\left(\frac{y(n) L}{L}\right) + 2y(n) L g'\left(\frac{y(n) L}{L}\right) L^{-1} \\
& = g(y(n)) + 2y(n) g'(y(n)) \\
& = n + \frac{2y(n)}{y'(n)} \qquad \text{since } g(\cdot) \text{ is inverse of } y(\cdot)
\end{aligned}$$

Recall $y'(n) = \frac{f(n)-y(n)}{n}$, so

$$\begin{aligned}
n + \frac{2y(n)}{y'(n)} & = n + \frac{2n y(n)}{f(n) - y(n)} \\
& = n \left(1 + \frac{2y(n)}{f(n) - y(n)}\right) \\
& = n \left(1 - \frac{2y(n)}{y(n) - f(n)}\right)
\end{aligned}$$

For $n > n_{MSY}$, $y(n) > f(n) \geq 0$, hence $\frac{2y(n)}{y(n)-f(n)} > 1$, so (8) – (9) < 0 , $h_{\bar{Q}} < 0$, and $\frac{dL^*}{d\bar{Q}} > 0$. ■

Proof of remaining comparative statics.

See table on page 15

As explained in the proofs the previous two comparative statics, the sign of the comparative static of n^* and L^* with respect to any exogenous variable x can be found by analyzing the sign of the relevant derivative of the first order condition, i.e.

$$\text{sign}\left(\frac{dn^*}{dx}\right) = -\text{sign}(g_x) \quad \text{and} \quad \text{sign}\left(\frac{dL^*}{dx}\right) = -\text{sign}(h_x)$$

We now present and sign the expressions of g_x for the parameters of interest.

$$g_{C_f} = -\frac{\bar{Q} \overbrace{y'(n^*)}}{y(n^*)^2} \qquad (> 0)$$

$$g_{C_n} = \underbrace{\frac{-\bar{Q}}{n^* y(n^*)}}_{-} \underbrace{\left[\frac{1}{n^*} + \frac{y'(n^*)}{y(n^*)}\right]}_{+} \quad (< 0) \qquad \text{Since } \varepsilon_{y(n^*)} > -1 \Rightarrow \frac{1}{n^*} + \frac{y'(n^*)}{y(n^*)} > 0 \quad (\text{Prop 2})$$

$$g_{C_D} = \underbrace{(1 - \alpha)}_{-} \bar{Q}^\alpha y(n^*)^{-\alpha} \underbrace{y'(n^*)}_{-} \quad (> 0)$$

$$\begin{aligned} g_\alpha &= -C_D \bar{Q}^\alpha y(n^*)^{-\alpha} y'(n^*) ((\alpha - 1)(\ln(\bar{Q}) - \ln(y(n^*))) + 1) \\ &= -\underbrace{C_D \bar{Q}^\alpha y(n^*)^{-\alpha}}_{+} \underbrace{y'(n^*)}_{-} \underbrace{((\alpha - 1)\ln(L) + 1)}_{+} \quad (> 0) \end{aligned}$$

We now present and sign the expressions of h_x for the parameters of interest.

$$h_{C_f} = L(n^*)^2 \quad (> 0)$$

$$h_{C_n} = Ln^* + \frac{\bar{Q}}{y'(n^*)} \quad (< 0) \quad \text{Since } \varepsilon_{y(n^*)} > -1 \Rightarrow Ln^* + \frac{\bar{Q}}{y'(n^*)} < 0 \quad (\text{Prop 2})$$

$$h_{C_D} = (\alpha - 1) (n^*)^2 \bar{Q} L^{\alpha-1} \quad (> 0)$$

$$h_\alpha = (n^*)^2 \bar{Q} C_D L^{\alpha-1} (1 + (\alpha - 1) \ln(L)) \quad (> 0) \Leftrightarrow L > e^{-1/(\alpha-1)}$$

■

B Calibration of the Cost-Minimization Problem

A piecewise linear spline function is used to estimate the age-yield function. With this functional form, the cost minimization problem has 9 parameters for which values must be found.

B.1 Brazilian Sugarcane

B.1.1 Piece-wise Linear Age-Yield Function: $t_1, t_{max}, t_T, f_{max}$

The piece-wise linear age-yield function has four parameters. Parameter t_1 designates the age at which the yield first becomes positive, t_{max} is the age at which maximum yield is achieved, and t_T is the age at which yield returns to zero. During the increasing

phase, between t_1 and t_{max} the function is a positive affine and during the decreasing phase, between t_{max} and t_T , the function is negative affine.

To estimate the parameters, we fit the linear-piecewise function to age-yield data obtained from Margarido and Santos (2012). Figure 6 shows the original data and the fitted age-yield function.

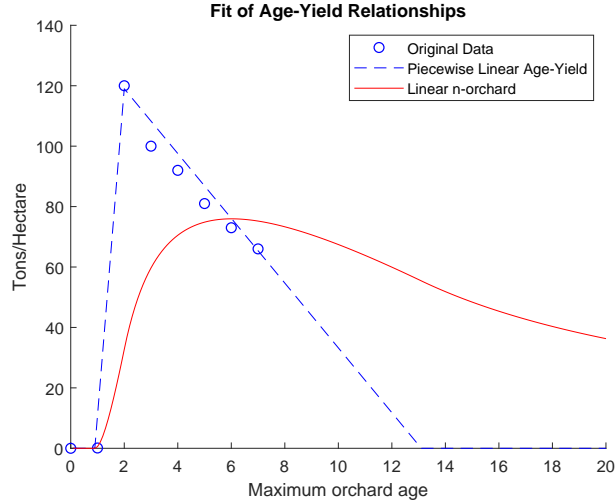


Figure 6: Fitting the piecewise-linear age-yield function to the Brazilian age-yield data from Margarido and Santos (2012).

The parameter values obtained are $t_1 = 1$, $t_{max} = 2$, $t_T = 13$, and $f_{max} = 120$.

B.1.2 Farm-gate Cost parameters: C_f , C_n

We derived the feedstock cost parameters, C_f and C_n , from Teixeira (2013), and the delivery cost parameter, C_D , from Crago et al. (2010).

Teixeira (2013) presents an example operating budget for a 5-cut (6-age-class) sugarcane operation in São Paulo state, where they assume that 80 percent of the cane is harvested burned, and 20 percent is harvested raw. Costs are divided into five categories, delivery costs, and four that account for farm gate feedstock costs: preparing the soil, planting, harvest, and maintenance of the ratoon. The total farm gate feedstock

costs for a 6 hectare operation is given by

$$\begin{aligned} \text{Total Farm Gate} \\ \text{Feedstock Costs} &= \text{Soil Preparation} + \text{Planting} \\ &+ 5 \times \text{Harvest} + 4 \times \text{Ratoon maintenance} \end{aligned}$$

Since the total cost is given for 6 hectares, the total cost per hectare is

$$\begin{aligned} \text{Total Farm Gate} \\ \text{Feedstock Costs} \\ \text{(Per Hectare)} &= \frac{1}{6} \times \text{Soil Preparation} + \frac{1}{6} \times \text{Planting} \\ &+ \frac{5}{6} \times \text{Harvest} + \frac{4}{6} \times \text{Ratoon maintenance} \end{aligned}$$

Assuming that these cost parameters are constant with respect to the number of age-classes we can write the total farm gate feedstock per hectare as a function of the age structure

$$\begin{aligned} \text{Farm gate} \\ \text{feedstock costs}(n) &= \frac{1}{n} \times \text{Soil Preparation} + \frac{1}{n} \times \text{Planting} \\ &+ \frac{n-1}{n} \times \text{Harvest} + \frac{n-2}{n} \times \text{Ratoon maintenance} \end{aligned}$$

Substituting Teixeira's numbers (in Reals) from the example budget, the cost function becomes

$$\text{Farm gate} \\ \text{feedstock costs}(n) = \frac{656.07}{n} + \frac{4159.83}{n} + \frac{n-1}{n} \times 1273.13 + \frac{n-2}{n} \times 986.54$$

Which on rearranging becomes

$$\text{Farm gate} \\ \text{feedstock costs}(n) = 2259.67 + \frac{1569.69}{n}$$

Hence for the simulations we use a baseline of $C_f = 2259.67$ and $C_n = 1569.69$.

B.1.3 Delivery Cost parameter: C_D

While Teixeira (2013) does include estimates of delivery costs, he does not include the processing facility size that this example farm is feeding. We therefore turn to Crago et al. (2010) to derive the delivery cost parameter.

The total delivery cost from a growing region is given by

$$\begin{aligned} \text{Total Delivery Costs} &= \text{Average Cost Per Ton Kilometer} \\ &\quad \times \text{Quantity Transported} \\ &\quad \times \text{Average Delivery Distance} \end{aligned}$$

Let δ represent the average delivery cost per ton kilometer (i.e. the average cost to transport one ton of feedstock one kilometer). Crago et al. (2010) report an average transport cost of R\$6.7 to transport a ton of feedstock from the farm gate to the mill. The average delivery distance in this study was 22 kilometers so in this case $\delta = 0.3045$.

The average mill size in Crago et al. (2010) is 4.8 million tons. Given our assumption that the growing region produces the exact quantity required to feed the mill, this implied that the average quantity of feedstock transported was 4.8 million tons.

When calculating the average delivery distance, we must make a distinction between the area of land planted with sugarcane, L , and the area of the growing region, A . Although we are assuming that the growing region is circular, it is not necessarily the case that all the land is planted with sugarcane. In fact, relaxing the link between planted area and growing region area is necessary to correctly calibrate the model to the data in Crago et al. (2010).

Let d be the average density of sugarcane fields in the growing region, and A be the area of the growing region. Hence

$$L = d \times A$$

The average delivery distance is given by the expression

$$r_{av} = \frac{2}{3}r_{max} = \frac{2}{3}\sqrt{\frac{A}{\pi}}$$

Since the average delivery distance, r_{av} , from Crago et al. (2010) is 22km, the size of the growing region is $A = 342\,119$ ha.

We calculate the density parameter from

$$\text{Total Quantity} = \text{Yield} \times \text{Density} \times \text{Growing Region Area}$$

Crago et al. (2010) reports an average yield of 75 tons per hectare. So we calculate the

density as

$$4800000 = 75 \times d \times 342119 \Rightarrow d = 0.187$$

Hence the expression for the total delivery cost becomes

$$\begin{aligned} \text{Total Delivery Costs} &= \delta \times Q \times r_{av} \\ &= \delta \times Q \times \frac{2}{3} \sqrt{\frac{A}{\pi}} \\ &= \delta \times Q \times \frac{2}{3} \sqrt{\frac{L}{d \times \pi}} \\ &= \frac{2\delta}{3} \sqrt{\frac{1}{d \times \pi}} \times Q \times \sqrt{L} \\ &= \frac{2\delta}{3} \sqrt{\frac{1}{d \times \pi}} \times y(n)L\sqrt{L} \\ &= \frac{2\delta}{3} \sqrt{\frac{1}{d \times \pi}} \times y(n)L^{1.5} \\ &= C_D \times y(n)L^{1.5} \end{aligned}$$

For the d and δ derived from Crago et al. (2010), $C_D = 0.2649$.

B.1.4 Growing area shape parameter, α

We assumed a circular growing area, which implies a value of $\alpha = 1.5$, as described above in the section on delivery costs.

B.2 Calibrated parameters and ranges used in simulations

	Parameter	Min Value	Calibration	Max Value
Yield	t_1	0	1	2
	t_{max}	$t_1 + 1$	2	$t_1 + 5$
	t_T	$t_{max} + 7$	13	$t_{max} + 13$
	f_{max}	60	120	180
Cost	C_f	1129.84	2259.67	3389.51
	C_n	784.85	1569.69	2354.54
	C_D	0.13	0.26	0.40
	α	0.75	1.50	2.25
Capacity	\bar{Q}	1 000 000	19 000 000	37 000 000

Table 3: Support for random parameters used in cost minimization. The parameters are drawn from a uniform distribution centered on the Brazilian calibration